An Architecture for Fluid/Structure Analysis of Turbomachinery Blading

David A. Johnston, Wright State University
Charles J. Cross, Air Force Research Laboratory
J. Mitch Wolff, Wright State University

10th National Turbine Engine High Cycle Fatigue Conference
March 8-11, 2005, New Orleans, Louisiana

Introduction

Aeroelastic stability and response analyses used in the design of turbomachinery blading are typically uncoupled: the unsteady aerodynamics and structural dynamics are treated in separate models, with boundary conditions sequentially updated after stationary periodic convergence is met. Higher fidelity simulations are achieved by coupling the fluid and structure domains such that boundary conditions are updated once or several times per physical time step of the simulation. Because of the rise and availability of faster, economical computational resources the time-marching, coupled-domain analysis, though still time consuming, is no longer deemed outright as impractical, but rather necessary to capture the behavior of certain aeroelastic systems. Carstens and Belz (2001) have shown that strong oscillating shocks and choked blade passage flow produce nonlinear interactions that are not well captured by uncoupled modeling. A coupled analysis in necessary to model limit cycle flutter (Gnesin et al., 2000) and to model some off-design, non-integral vibration problems to assess whether the unsteady flow will lock-in to any of the natural frequencies of nearby blade rows (Silkowski et al., 2002).

To enhance the Air Force Research Laboratory, Propulsion Directorate's in-house research computational tools, a computer software code with the working name, *FSI*, is in development to analyze with high fidelity the transient fluid/structure interaction of elastic blade rows in turbomachinery. The code is designed to leverage existing computational fluid dynamics (CFD) and computational structural dynamics (CSD) software, therefore, the so-called partitioned approach (Piperno et al., 1995; Matthies and Steindorf, 2003) is taken. As a starting point, the turbomachinery CFD research code *TURBO* (Chen and Briley, 2001) and the commercial structural solver *ANSYS*® has been chosen for coupling, although *FSI* is designed with modularity for future inclusion of other fluid and structural solvers. This extended abstract will highlight the design of the fluid/structure interaction code and present the results of some simulations used to validate it.

Code Overview

Coupled fluid/structure interaction algorithms can be classified as either monolithic or partitioned. With the monolithic method the fluid and structure domains are discretized into a single arbitrary Lagrangian-Eulerian space and solved at each time step using a single integrator. With the partitioned method the fluid and structure domains are modeled and solved separately, but information is exchanged once or several times per time step to update the boundary conditions of each domain. Because of the following

advantages, the partitioned approach was chosen over the monolithic approach for the design of *FSI*. The partitioned approach permits the use of existing, mature solvers for each domain and permits the independent modeling by analysts in their domain of specialty and with familiar tools. Further, the partitioned approach enables the customization of the solver for each domain.

FSI orchestrates the flow of information between the two domains, performing node mapping between the two domains at the interface, integration of the fluid stress tensor for aero load boundary conditions to the structural model, and deformation of the fluid mesh based on the structural deflection of the blades.

Information Flow

The flow of information is depicted in Fig. 1, where the completion of one cycle can occur once or several times per time step depending on the user-specified degree of coupling. Essentially the fluid stress tensor provided by the fluid solver is integrated over the wetted surface (i.e., fluid/structure interface) to yield the instantaneous aero load acting on the structure. With these boundary conditions the structure solver converges to provide displacements. Those at the wetted surface are projected into the fluid mesh, smoothly deforming it. New metrics are calculated for the deformed mesh and the fluid solver is run to convergence, completing one cycle. Accuracy is increased by decreasing the time step or by inter-domain iteration at a given time step. The latter method is usually computationally more expensive than the former.

The *FSI* code manages the flow of information between the fluid and structure solvers through an Internet domain, connection-oriented, server/client socket, depicted in Fig. 2. As shown in this example, the socket is established between the master fluid processor P0 and the master structure processor P3, all operating on a Beowulf cluster of direct memory processors (Buyya, 1999). Master processors communicate to worker processors via the MPI protocol (Message Passing Interface Forum, 1994). Thus both solvers are parallelized via domain decomposition.

Mapping

Boundary conditions at the fluid/structure interface G require that the fluid and structural stresses s be in equilibrium and that the displacement fields d be compatible,

$$\vec{s}_S \cdot \vec{n} = \vec{s}_F \cdot \vec{n} \quad \text{on } G \qquad (1)$$

$$\vec{d}_S = \vec{d}_F \quad \text{on } G \qquad (2)$$

Enforcing these conditions requires that a mapping be performed between the fluid mesh and the structural mesh at the interface, whereby each fluid node is associated with one and only one structural element for displacement transfer and each structural element is associated with one or more fluid nodes for load transfer.

The mapping is achieved in three passes. In the first pass an alternating digital tree search is performed (Bonet and Peraire, 1991) to locate all fluid nodes at the interface that are near a given structural element. The search is fast as it operates with order $N \log_2 N$ time, where N is the total number of fluid nodes at the interface. A second pass comprises a point-in-polygon test which is made to eliminate false positives, i.e., fluid nodes that are near the element, but not near enough to fall within the user-specified geometric tolerance. Finally, a third pass is made to resolve the degenerate cases of a fluid node associated with many structural elements (produced by concavity of the structure) or associated with zero structural elements (produced by convexity of the structure).

In the example shown in Fig. 3, the first pass associates fluid nodes B and C with the structural element bounded by the volume of dashed lines. The second pass retains only fluid node B with the structural element bounded by the shaded volume. The lower portion of the figure illustrates structural concavity and convexity that produces multi- and zero associations, that are resolved in the third pass.

The mapping is a preprocessing operation performed only once for a given set of structure and fluid meshes.

Load Transfer

The fluid stress tensor is integrated by Gauss quadrature to determine the aero loading at a given fluid node. Bilinear shape functions from finite element theory are used to evaluate the stress tensor at the Gauss points using a choice of either full or reduced integration (Bathe, 1996). The area of integration is circumscribed using the locations of the fluid cell face centroids, cell wall midpoints, and mesh points. In this way quadrilateral facets are formed independent of the type of polygon that forms the fluid cell face, permitting a single algorithm to be used independent of the fluid cell shape. Four facets (dashed lines) form the area of integration for the center fluid node in Fig. 4. To the right is an enlargement of one facet, shown with four Gauss integration points (crosses).

The loading of the interface fluid nodes is conservatively transferred to the interface structural nodes using shape functions (Farhat et al., 1998). *FSI* employs 2-D, isoparametric shape functions based on the structural element face at the interface. Figure 5, schematically depicts this transfer, where fluid and structural nodal force vectors are F and f, respectively. The transfer example depicted in the figure is governed by Eqn. 3, where $N(x)$ is the shape function. (Subscripts identify nodes rather than vector components.)

$$f_i = \sum_{j=1}^{3} N_i(x_j) F_j \quad i = 1,2 \qquad (3)$$

Displacement Transfer

The same shape functions are again used to transfer the computed structural node displacements at the interface to the fluid nodes at the interface. The interpolation process is illustrated in Fig. 6 and governed by Eqn. (4), where fluid and structural node displacement vectors are D and d, respectively.

$$D_j = \sum_{i=1}^{2} N_i(x_j) d_i \quad j = 1,2,3 \qquad (4)$$

An algebraic method for structured fluid meshes (Morton et al., 1998) is used to project the interface displacement smoothly into the interior of the fluid mesh, deforming it so as to maintain the original mesh quality, yet body-fitted to the new blade position. Anchor points are defined some distance away from the blade. The locus of anchor points forms a closed surface within which the mesh deforms, Fig. 7. The method operates on lines of constant computational coordinate, beginning with the point touching the blade and ending at the anchor point. The method steps are schematically presented at the lower portion of the figure. The blade displacement is applied to all points on the line, translating the mesh line from (1) to (2). An arc length based Hermite function blends lines (1) and (2), forming the final mesh line (3). To reduce possible fluid cell shearing, the method was modified for application near the blade tip region such that the anchor point is changed to a sliding point that is free to move along the hub or case wall surface.

Validation: Helical Fan

The helical fan test case (Montgomery and Verdon, 1997) is used to validate *FSI*. In this case, *FSI* is run in specified-motion mode and coupled to *TURBO*. The motion is prescribed to be rigid-body plunge at unity reduced frequency and zero interblade phase angle. This case exercises approximately eighty percent of the *FSI* code. (Only that portion which interacts with the structure solver is not exercised by this case). Figure 8 shows the midspan computational domain in the form of a Mach contour plot. The helical fan is formed of zero thickness, flat plate blades with twist, and having a midspan stagger of 45 deg. In Fig. 9, the midspan unsteady loading prediction shows good agreement with the linear theory predictions of the *LINSUB* analysis (Whitehead, 1987).

Validation: Standard Configuration 4

The three-dimensional version of the Fourth Standard Configuration, Stcf4, (Bölcs and Fransson, 1986) is used to validate *FSI* coupling *TURBO* with *ANSYS*. For this case, the interblade phase angle is –90 deg, therefore, four blade passages were modeled, Fig. 10. The configuration features turbine airfoils of high blade thickness and camber operating under high subsonic flow conditions.

To match the experiment, *FSI* was executed in the specified-motion mode using the first bending mode prediction from an *ANSYS* modal analysis of the blade cantilevered from the hub wall. This is in contrast to the experiment, wherein the blades vibrated cantilevered from a spring support inboard of the hub wall, more like a rigid-body plunge mode, but not quite. The displacement amplitude at midspan was matched to that of the experiment. The simulation was started from a converged steady-state solution and ran at 200 time steps per cycle for ten vibration cycles to achieve periodic convergence. The unsteady pressure coefficient amplitude comparison is shown in Figure 11. The pressure surface predictions are better than those of the suction surface. The suction surface is overpredicted in the midchord region by as much as a factor of 2.8 and appears to correlate with the poor matching of the steady-state pressure coefficient in that same region. Because the steady-state predictions are made without *FSI*, the quality of prediction seems to lie with the *TURBO* modeling rather than *FSI*. Additional work in the form of fluid mesh refinement and incidence adjustment is required to attempt a better match to the time-average and unsteady data.

To validate *FSI* coupling *TURBO* with *ANSYS* in the fluid/structure interaction mode, the four blade passages of the fluid model where coupled with four structural models of the associated blades cantilevered to the hub wall. (This case exercises one hundred percent of the *FSI* code.) *ANSYS* was run using the Newmark method time integration. The coupled analysis was started from a converged CFD solution, but the structure was started with a step function from zero loading to the converged CFD solution loading in order to excite many structural modes. The time trace of incremental work of air acting on each blade was captured over ten periods of the first bending mode vibration, with 400 time steps per period and one information exchange per time step. Figure 12 presents a Fourier spectrum of the incremental work time trace of blade 1. The participation of bending, torsion, and the stiffwise bending vibrational modes are evident and identified by correlating the frequencies of the spectrum peaks to the *in vacuo* modal frequencies predicted in an *ANSYS* modal analysis of the blade. Therefore, it is reasoned that *FSI* is properly orchestrating the interaction of the two coupled domains, providing a time-marching simulation of the aeroelastic system.

Reference

Bathe, Klaus-Jürgen, 1996, *Finite Element Procedures*, Chapter 5, (Prentice Hall: New Jersey).

Bölcs, A., and T. H. Fransson, 1986, "Aeroelasticity in turbomachines comparison of theoretical and experimental cascade results," Communication No. 13, L'École Polytechnique Fédérale de Lausanne (EPFL), Switzerland.

Bonet, Javier, and Jaime Peraire, 1991, "An alternating digital tree (ADT) algorithm for 3D geometric searching and intersection problems," *International Journal for Numerical Methods in Engineering*, Vol. 31, pp. 1–17.

Buyya, Rajkumar, 1999, *High Performance Cluster Computing: Vol. 2*, Chapter I: Programming Environments and Development Tools, (Prentice-Hall: New Jersey).

Carstens, V., and J. Belz, 2001, "Numerical investigation of nonlinear fluid-structure interaction in vibrating compressor blades," *ASME Journal of Turbomachinery*, Vol. 123, No. 2, pp. 402–408.

Chen, J. P., and W. R. Briley, 2001, "A parallel flow solver for unsteady multiple blade row turbomachinery simulations," ASME paper 2001-GT-0348.

Farhat, C., M. Lesoinne, and P. LeTallec, 1998, "Load and motion transfer algorithms for fluid/structure interaction problems with non-matching discrete interfaces: Momentum and energy conservation, optimal discretization and application to aeroelasticity," *Computer Methods in Applied Mechanics and Engineering*, Vol. 157, pp. 95–114.

Gnesin, V., R. Rzadkowski, and L. Kolodyazhnaya, 2000, "A coupled fluid-structure analysis for 3D flutter in turbomachines," ASME paper 2000-GT-380.

Matthies, Hermann G., and Jan Steindorf, 2003, "Partitioned strong coupling algorithms for fluid-structure interaction," *Computers & Structures*, Vol. 81, pp. 805–812.

Message Passing Interface Forum, 1994. *MPI: A Message-Passage Interface Standard*. www.mpi-forum.org

Montgomery, Matthew D., and Joseph M. Verdon, 1997, "A three-dimensional linearized unsteady Euler analysis for turbomachinery blade rows," NASA Contractor Report 4770.

Morton, Scott A., Reid B. Melville, and Miguel R. Visbal, 1998, "Accuracy and coupling issues of aeroelastic Navier-Stokes solutions on deforming meshes," *Journal of Aircraft*, Vol. 35, No. 5, pp. 798–805.

Piperno, S., C. Farhat, and B. Larrouturou, 1995, "Partitioned procedures for the transient solution of coupled aeroelastic problems," *Computer Methods in Applied Mechanics and Engineering*, Vol. 124, pp. 79–112.

Silkowski, P. D., C. M. Rhie, G. S. Copeland, J. A. Eley, and J. M. Bleeg, 2002, "Computational-fluid-dynamics investigation of aeromechanics," *AIAA Journal of Propulsion and Power*, Vol. 18, No. 4, pp. 788–796.

Whitehead, D., 1987, "Classical Two-Dimensional Methods," *Manual on Aeroelasticity in Axial-Flow Turbomachinery: Unsteady Turbomachinery Aerodynamics*, M. F. Platzer and F. O. Carta, eds., Vol. 1, AGARDograph No. 298.

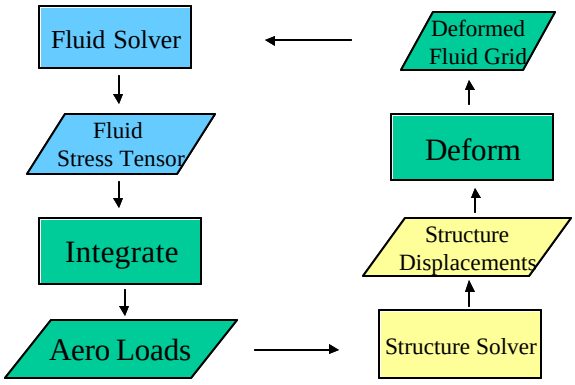

Figure 1 Flow of information.

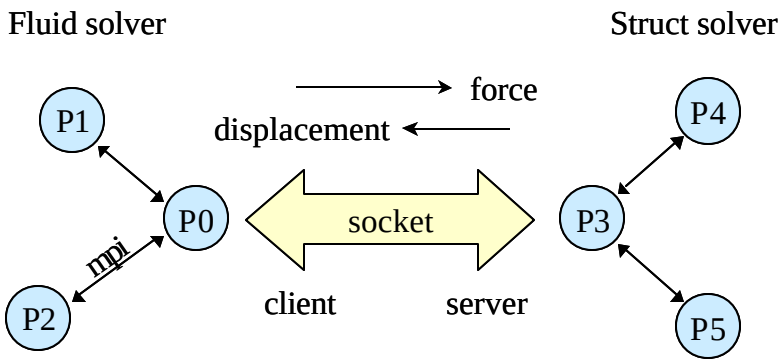

Figure 2 Socket communication.

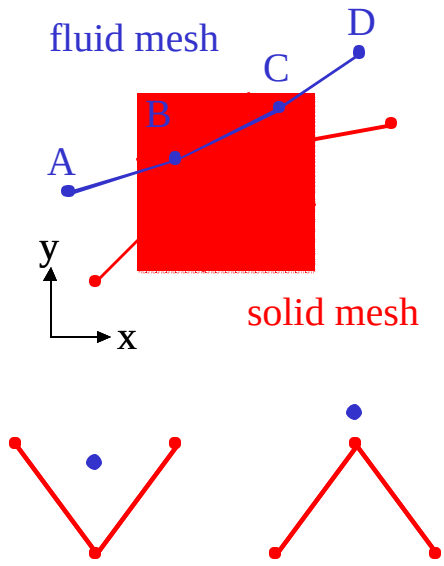

Figure 3 Mapping of the fluid and structural meshes at the interface.

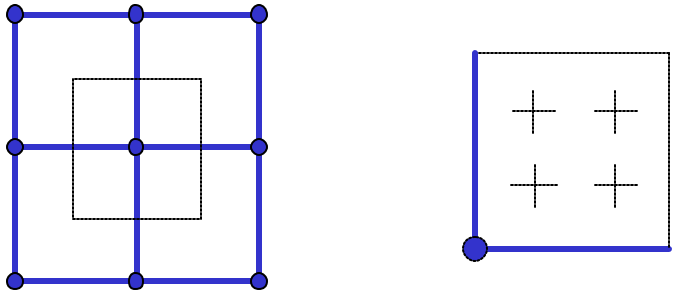

Figure 4 Area for Gauss quadrature.

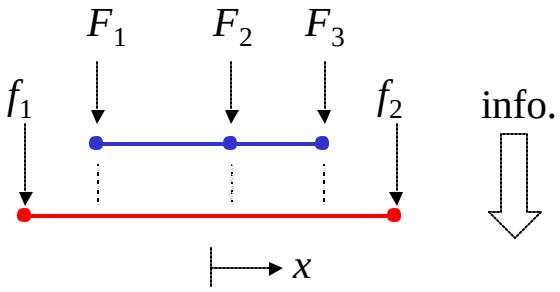

Figure 5 Conservative transfer of forces from fluid mesh to structural mesh.

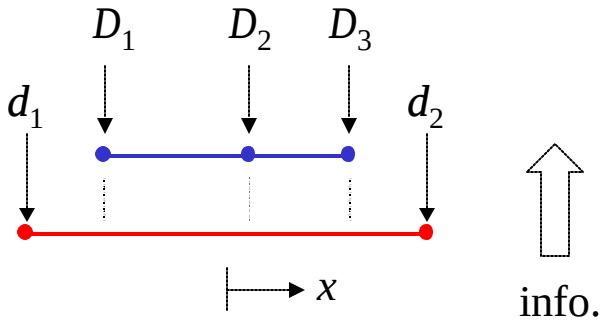

Figure 6 Interpolative transfer of displacements from structural mesh to fluid mesh.

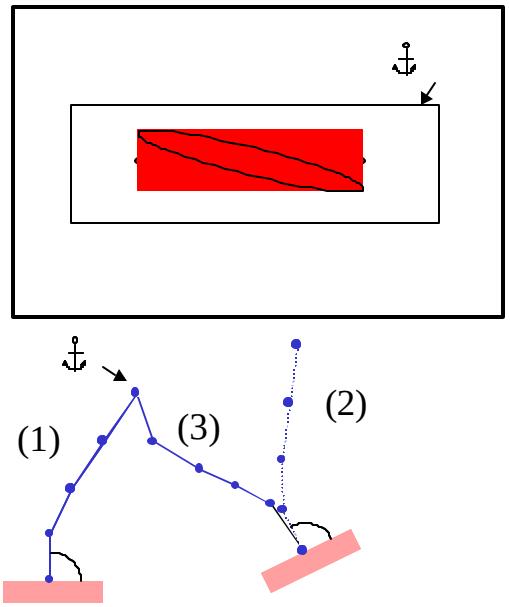

Figure 7 Algebraic fluid mesh deformation.

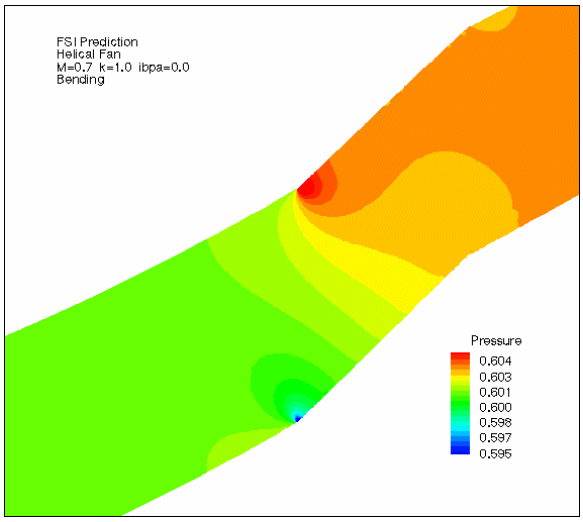

Figure 8 Helical fan domain.

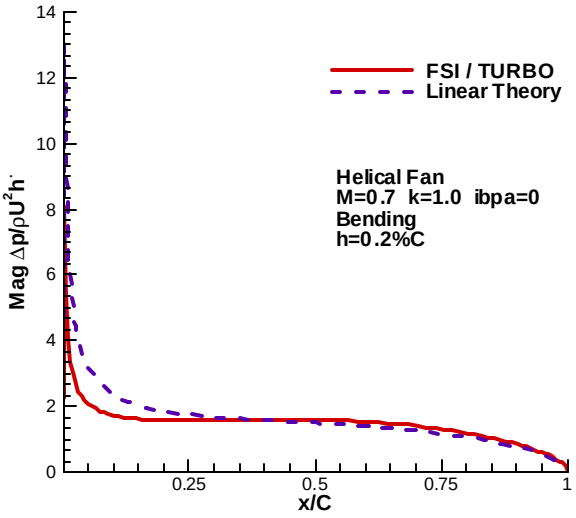

Figure 9 Helical fan unsteady pressure coef.

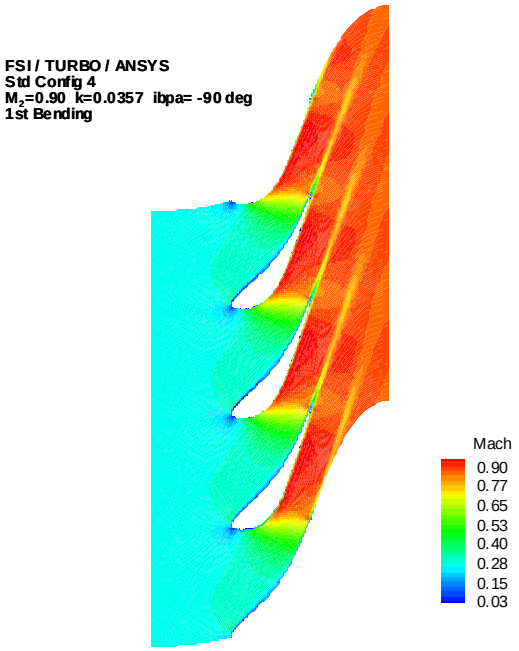

Figure 10 Stcf4 domain.

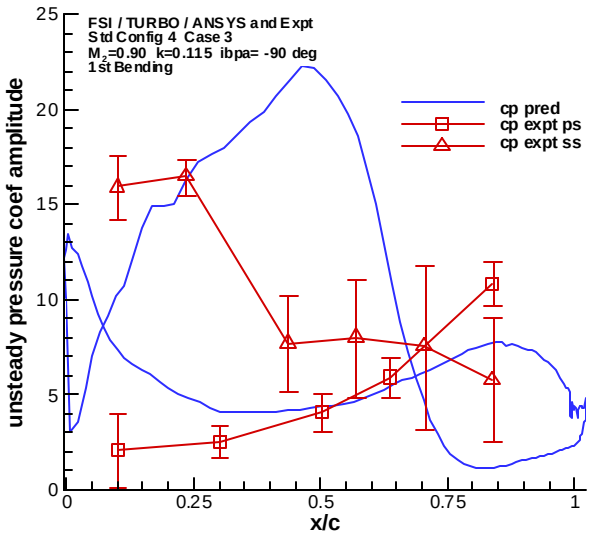

Figure 11 Stcf4 unsteady pressure coef.

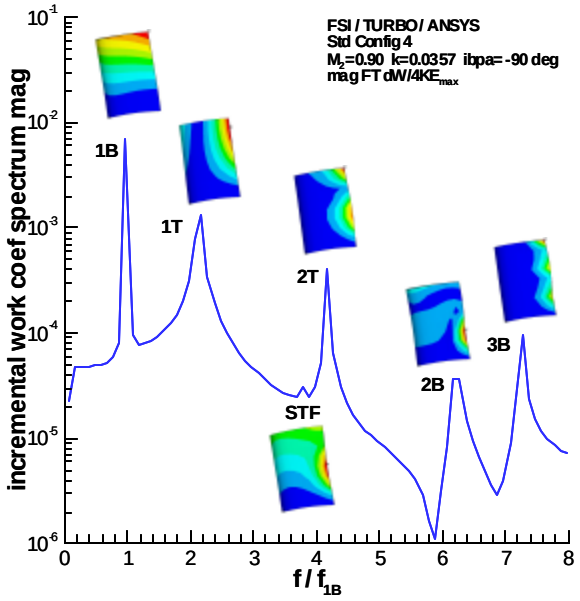

Figure 12 Fourier spectrum of incremental work indicating mode participation.